Chapter 4

Interacting Populations: Competition, Predation, and Parasitoids

Even in simple one-species unstructured models we have seen the potential for stability, cycles or chaos. In this chapter we consider another potential source of complex dynamics: interactions between different species. We will examine a series of models for different kinds of interactions, along the way learning the techniques for dealing with multi-species models. As in the last chapter, we will continue (for now) to use unstructured models that ignore within-species differences between individuals. We start with models in continuous time, and then consider discrete-time models.

4.1 Lotka-Volterra Competition Model

The Lotka-Volterra models are the extension to multiple species of the single-species logistic model. That is, the state variables are the total density of each species, and the per-individual effects are linear – the effect of species i on the per-capita growth rate of species j is proportional to the density of the species. In studying these models, we don't really believe the assumption of linearity – but it's the natural starting point, and it gives you the right "picture" for thinking about more general models.

The model for two competing species is

$$\begin{aligned} \dot{N}_1 &= r_1 N_1 \left(1 - \frac{N_1}{K_1} - \beta_{12}\frac{N_2}{K_1}\right) \\ \dot{N}_2 &= r_2 N_2 \left(1 - \frac{N_2}{K_2} - \beta_{21}\frac{N_1}{K_2}\right). \end{aligned} \tag{4.1}$$

Each β_{ij} is a positive parameter measuring the relative impact of one species j individual on the growth

of species i, relative to the impact of one species i individual.

The model is only interesting if each species could persist in the absence of the other, which means $r_1, r_2 > 0$. In that case we can't have both species going extinct – for if we did, then each species would eventually have $\dot{N}_i/N_i > 0$ and it would then be increasing rather than decreasing. The possible outcomes in the model are then persistence of both species, or persistence of one while the other goes to extinction.

We can get a complete picture of this model's behavior by examining its *nullclines*. The nullclines are the curves in the (N_1, N_2) plane where $\dot{N}_i = 0$. Nullclines have two important properties:

- Solution curves cross the N_1 nullcline going vertically up or down, because at that location only N_2 is changing. They cross the N_2 nullcline going horizontally to the left or the right.
- So long as $\dot{N}_1$ and $\dot{N}_2$ are continuous functions of (N_1, N_2) the sign of $\dot{N}_i(N_1, N_2)$ can only change when you cross the N_i nullcline.

For the Lotka-Volterra competition model the nullclines are

$$\begin{aligned} \dot{N}_1 = 0: &\quad N_1 = 0 \text{ or } \frac{N_1}{K_1} + \beta_{12}\frac{N_2}{K_1} = 1 \\ \dot{N}_2 = 0: &\quad N_2 = 0 \text{ or } \frac{N_2}{K_2} + \beta_{21}\frac{N_1}{K_2} = 1 \end{aligned} \tag{4.2}$$

The second condition in each nullcline defines a line with negative slope in the first quadrant of the (N_1, N_2) plane. Any intersection of the nullclines is a fixed point, so there are potentially four fixed points:

$$(0,0), (K_1, 0), (0, K_2), (N_1^*, N_2^*), \tag{4.3}$$

the last existing if the off-axis parts of the nullclines intersect.

The nullclines are lines, so they are determined by their points of intersection with the axes:

The N_1 nullcline runs from $\left(0, \dfrac{K_1}{\beta_{12}}\right)$ to $(K_1, 0)$.

The N_2 nullcline runs from $(0, K_2)$ to $\left(\dfrac{K_2}{\beta_{21}}, 0\right)$.

There are four possible configurations of the nullclines, depending on which of them has the higher intersection with the N_2 axis, and which of them has the rightmost intersection with the N_1 axis.

Consider first the case where the N_2 nullcline lies entirely above the N_1 nullcline. From the differential equations, we see that each $\dot{N}_i$ is negative above the nullcline for that species, and positive below it. That tells us the direction of flow for solution curves in each region of the positive quadrant (Figure 4.1).

Looking at the directions of flow, we should suspect that all nonzero solutions tend to $(0, K_2)$ – species 2 wins – and we can prove it. Consider first a solution starting about the N_2 nullcline. If the solution never

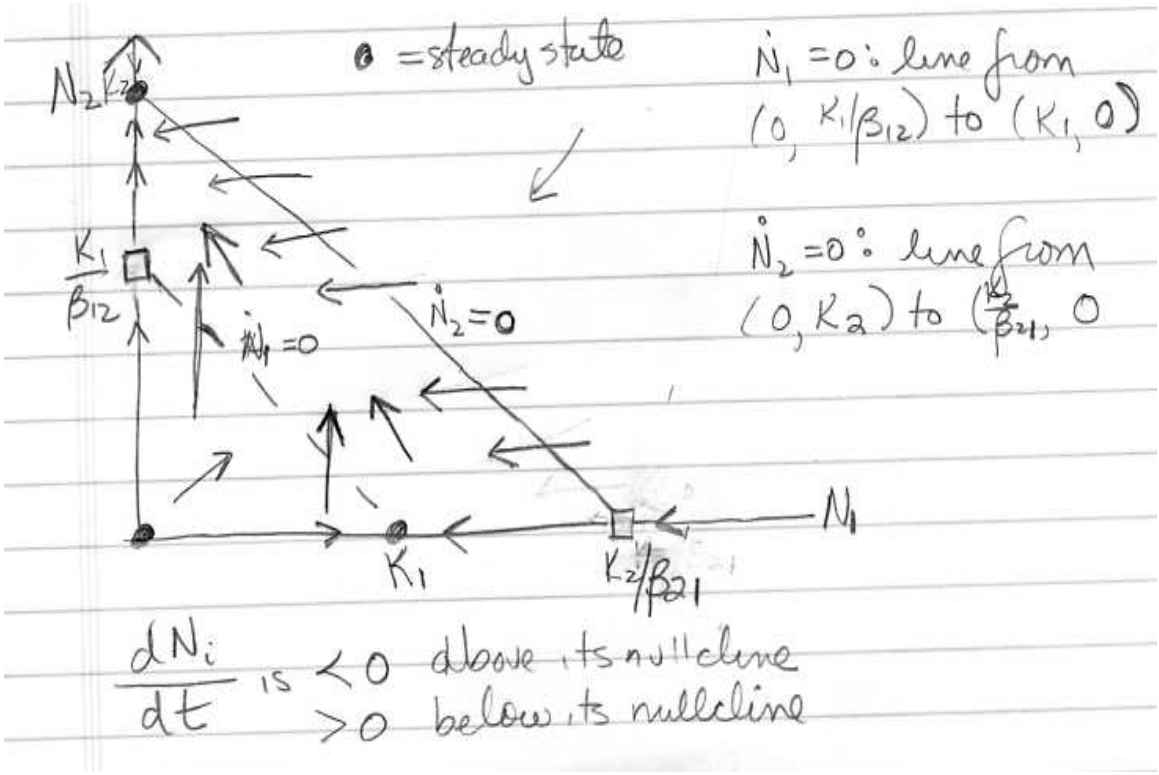

Figure 4.1: Nullclines in the Lotka-Volterra competition model, when the N_2 nullcline lies entirely above the N_1 nullcline. Arrows indicate the direction of flow implied by the nullclines.

crosses the N_2 nullcline, then N_1 and N_2 are monotonically decreasing and therefore converge to limiting values. Convergence to a limit means that $\dot{N}_i \to 0$, so the limit must be a fixed point. The only possible limit point is therefore $(0, K_2)$. If the solution does cross the N_2 nullcline, it can never escape the region between the nullclines. Therefore, once it enters that region N_1 is monotonically decreasing and N_2 is monotonically increasing. So again the solution must approach a limit that must be an equilibrium, which must be $(0, K_2)$.

We've already shown that a solution starting between the nullclines converges to $(0, K_2)$. A solution starting below the nullclines (but not at $(0, 0)$) must either remain below the nullclines (and therefore increase monotonically to a limit that must be $(0, K_2)$) or else cross into the region between the nullclines.

If the N_1 nullcline lies entirely above the N_2 nullcline – just swap $1 \leftrightarrow 2$ and we have the species 1 wins, and $N_2 \to 0$. The cases where the nullclines cross are slightly different, but the style of argument is the same: so long as solutions don't cross a nullcline they are monotonic increasing or decreasing, so solutions curves must converge to a limit, and the limiting point must be an equilibrium. The nullcline configurations and the conclusions are shown in Figure 4.2.

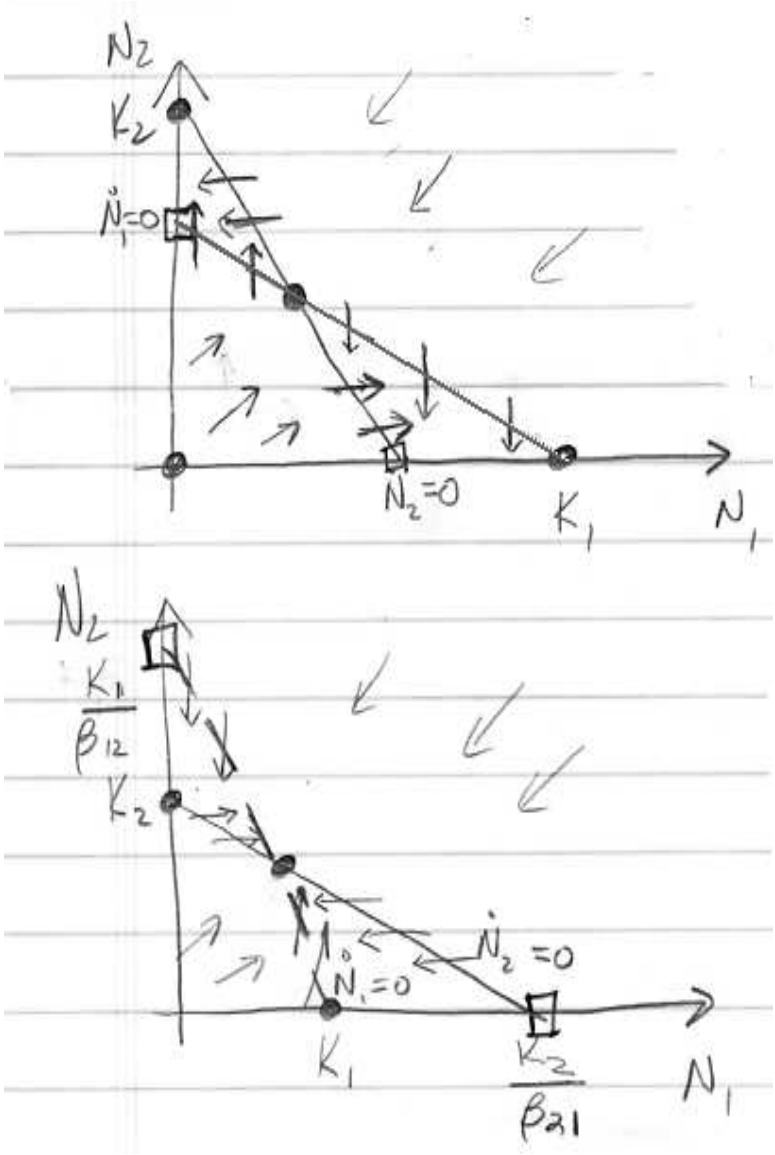

Figure 4.2: Nullclines in the Lotka-Volterra competition model, for the cases where the nullclines cross. Arrows indicate the direction of flow implied by the nullclines. In the upper panel there is contingent exclusion – one or the other goes extinct, depending on initial conditions – and in the bottom there is coexistence.

So coexistence of both species occurs only when

$$\begin{aligned} &\frac{K_2}{\beta_{21}} > K_1 \iff \frac{1}{K_1} > \frac{\beta_{21}}{K_2} \\ &\text{and} \\ &\frac{K_1}{\beta_{12}} > K_2 \iff \frac{1}{K_2} > \frac{\beta_{12}}{K_1} \end{aligned} \tag{4.4}$$

We can say this in words: coexistence occurs when within-species effects of density – the impact of one individual on the per-capita growth rate of its own species – is larger than the between-species effect.

Exercise 4.1 [from Hastings 1997] One nonobvious prediction of the Lotka-Volterra competition model is that nonselective mortality – "rarefaction" – can permit coexistence when there would otherwise be competitive exclusion. That is, consider the model

$$\begin{aligned} \dot{N}_1 &= r_1 N_1(1 - N_1/K_1 - \beta_{12} N_2/K_1) - mN_1 \\ \dot{N}_2 &= r_2 N_2(1 - N_2/K_2 - \beta_{21} N_1/K_2) - mN_2 \end{aligned} \tag{4.5}$$

(a) Find the equations for the nullclines in this model.
(b) Show, by plotting nullclines, that there are parameter values such that exclusion occurs for $m = 0$, but that coexistence occurs when m is increased to a suitable positive value (e.g. by experimental removals) with all other parameters remaining the same.

4.2 Mechanistic competition models

Although historically important and influential, the Lotka-Volterra models are now viewed as *phenomenological* because the interspecific effects are imposed without regard to the underlying mechanism – we simply posit that for some unspecified reason each species impedes the other's growth by some amount. Some argue that Lotka-Volterra models therefore should be totally discarded; others still use them as the basis for modeling multispecies interactions; but virtually all agree that it is preferable to use models based explicitly on the mechanisms of interaction, whenever possible. In this section we discuss two examples: competition for resources, and competition for space.

4.2.1 Competition for resources

Suppose that two species are both limited by some one resource that is in short supply, all other resources being relatively more abundant. We can model this mechanistically by adding resource abundance (R) as a state variable in the model. For example,

$$\begin{aligned} \dot{n}_1 &= \chi_1 f_1(R) n_1 - d_1 n_1 \\ \dot{n}_2 &= \chi_2 f_2(R) n_2 - d_2 n_2 \\ \dot{R} &= R_0 - f_2(R) n_1 - f_2(R) n_2 - \delta R \end{aligned} \tag{4.6}$$

Here d_1, d_2 are the per-capita death rates of the species, f_1, f_2 are their per-capita rates of nutrient uptake, and χ_1, χ_2 are the conversion rates between nutrient uptake and offspring production. The limiting is supplied at rate R_0 and degrades (or is lost) at rate δ. This model is *well-mixed* – we don't take account of spatial variability in resource availability or the density of the two species.

More species (e.g. grazers) or multiple nutrients can be included. Aquatic ecologists place great faith in such models because they have fared remarkably well in experimental tests using laboratory-scale

microcosms with plankton species (e.g., Tilman 1982, Fussmann et al. 2000). A classic result for the simple two-species, one-nutrient model is that you always have competitive exclusion:

> Let R_1^*, R_2^* be the nutrient levels at which each species can just barely survive ($\chi_i f_i(R_i^*) = d_i$). Then whichever species has the lower R^* drives the other to extinction.

Thus, coexistence of competitors must involve more than one limiting resource. Tilman, Matson, and Langer (1981) measured the R^*'s for silica of two species of freshwater diatoms (*Asterionella formosa, Synedra Ulna*) by growing each separately in a laboratory system corresponding to the model above with only one species at a time present, and waiting for it to reach equilibrium (at which point $R = R^*$ for the species). They found that *Synedra* had the lower R^*. Subsequent experiments confirmed that with both species in the system, regardless of the initial population densities, *Synedra* drove *Ulna* to extinction. Tilman (1982) reports similarly good results for predictions of coexistence versus exclusion in systems with more than one limiting nutrient.

Exercise 4.2 (a) To the resource-competition model above, add a *toxin* – a chemical that each species releases (at a species-specific per-capita rate), and which has a detrimental effect on both of the species. Let L denote the toxin concentration (i.e. we assume that both species are releasing the same toxic substance) and assume that each species' death rate is an increasing function of L (though the impact of L is not necessarily the same on each species). Write out and explain a system of differential equations corresponding to these assumptions. (b) Do you think it might be possible for two species to coexist in the model with a toxin? Why, or why not?

4.2.2 Competition for space

Sessile or territorial organisms require a unit of space or substrate in order to complete their life cycle and reproduce. Population growth is then limited by the availability of such "sites". Suppose that there are N sites available (e.g. room for N adult barnacles on a stretch of rocky shoreline), and two species in a strict competitive hierarchy. [This example and the exercises are mostly taken from Hastings (1997)]

Species 1 is the top competitor, and as far as it is concerned there is no difference between an empty site and one occupied by species 2. Its dynamics are

$$\dot{n}_1 = M_1 n_1 (N - n_1) - e n_1$$

representing a balance between colonization of new sites (empty or occupied by species 2) and extinction of occupied sites. The colonization model implicit in this equation is that each established individual of species 1 has probability M_1 per unit time of having an offspring land in a given site, which it then occupies unless some other individual of species 1 is already in the site.

For species 2, a site occupied by species 1 is not available for colonization, so

$$\dot{n}_2 = M_2 n_2 (N - n_1 - n_2) - e n_2 - M_1 n_1 n_2$$

Here the last term represents the rate at which species 1 takes over sites occupied by species 2.

Exercise 4.3 Show how the model above can be rescaled into the form

$$\begin{aligned} \dot{x}_1 &= m_1 x_1(1 - x_1) - e x_1 \\ \dot{x}_2 &= m_2 x_2(1 - x_1 - x_2) - e x_2 - m_1 x_1 x_2 \end{aligned} \tag{4.7}$$

and give expressions for the x_i and m_i in terms of the original model variables and parameters. [Note: we could scale out one more parameter, but for interpreting the results of the following exercises it's better not to].

Exercise 4.4 Find the nonzero equilibrium for the dominant species by setting $\dot{x}_1 = 0$. What conditions on the parameters are necessary for the equilbrium to be positive? Give an intuitive interpretation.

Exercise 4.5 Assuming parameter values such that the dominant competitor can survive, find the nonzero equilibrium for species 2 by substituting the equilibrium value for x_1 into $\dot{x}_2$ and solving for the value of x_2 that makes $\dot{x}_2 = 0$. What must be true about the relative values of m_1 and m_2 for both species to persist? Does this make intuitive sense?

Exercise 4.6 Suppose that parameters are such that both species can coexist, but the extinction rate e is then slowly increased. Which species goes extinct first (i.e., which has its positive equilibrium become negative at the lower value of e)?

4.2.3 Competition for light

Jef Huisman and colleagues (see citations at the end of this chapter) have developed and tested a mechanistic theory of competition for light among light-limited plankton. Although similar in many ways to resource competition theory, these models also take account of the spatial variability of light, in particular its depth-dependence in the water column and how that is affected by the abundance of the competing species. **more needed here**.

4.3 Local stability analysis: continuous time

Nullclines don't always tell us the whole story. More often we need to use local stability analysis. For multi-species models this requires a bit of matrix and vector algebra, which is reviewed in the Appendix at the end of this chapter.

Local stability analysis for models with more than one state variable is based on a multivariate Taylor series. For two variables, the leading terms in the series are

$$f(x_1 + e_1, x_2 + e_2) = f(x_1, x_2) + e_1 \frac{\partial f}{\partial x_1} + e_2 \frac{\partial f}{\partial x_2} + \cdots \tag{4.8}$$

where the derivatives are evaluated at (x_1, x_2), and $\cdots$ indicates higher order terms in the deviations

e_1, e_2. Similarly with m state variables

$$f(x_1 + e_1, x_2 + e_2, \cdots, x_m + e_m) = f(x_1, x_2) + e_1 \frac{\partial f}{\partial x_1} + e_2 \frac{\partial f}{\partial x_2} + \cdots + e_m \frac{\partial f}{\partial x_m} + \cdots \tag{4.9}$$

We now apply this to a general multispecies model

$$\dot{n}_i = f_i(n_1, n_2, \cdots n_m) = f_i(n), \qquad i = 1, 2, \cdots, m \tag{4.10}$$

An equilibrium occurs at $\hat{n}$ where all $f_i(\hat{n}) = 0$.

Let $x_i = n_i - \hat{n}_i \qquad \Rightarrow \dot{x}_i = \dot{n}_i = f_i(n) = f_i(\hat{n} + x)$ We now use Taylor series to approximate $f_i(\hat{n} + x)$ using the fact that $f_i(\hat{n}) = 0$. The resulting equation for the local dynamics is

$$\dot{x}_i = \sum_j \frac{\partial f_i}{\partial n_j} x_j \tag{4.11}$$

where the derivatives are evaluated at $\hat{n}$. The sum in the last equation has the form of a matrix-vector multiplication. We therefore define the *Jacobian matrix* $\mathbf{J}$ by

$$\mathbf{J}[i, j] = \frac{\partial f_i}{\partial n_j} \text{ evaluated at } \hat{n}. \tag{4.12}$$

The local dynamics are therefore the linear system

$$\dot{x} = \mathbf{J}x. \tag{4.13}$$

How does this system behave?

Consider a linear system $\dot{x} = \mathbf{A}x$, with equilibrium $\hat{x} = 0$. In the 1-variable case ($\dot{x} = ax$) we get exponential solutions, $e^{at}x(0)$. In the multivariable case, we get something similar from the eigenvectors and eigenvalues of the matrix $\mathbf{A}$. Recall the definition:

λ is an eigenvalue of $\mathbf{A}$, and $w \neq 0$ a corresponding eigenvector, if $\mathbf{A}w = \lambda w$.

Note that eigenvectors are only defined up to constant: if w is an eigenvector for $\mathbf{A}$ so is cw for any constant $c \neq 0$. The requirement that $w \neq 0$ is important. Without it any number c would be an "eigenvalue" corresponding to $w = 0$, because $\mathbf{A}0 = c0 = 0$.

Eigenvectors are important because they give exponentially growing or decaying solutions, $x(t) = e^{\lambda t}w$. This can be demonstrated by direct substitution:

$$\begin{aligned} \dot{x} &= \lambda e^{\lambda t} w \\ \mathbf{A}x &= e^{\lambda t}\mathbf{A}w = e^{\lambda t}\lambda w = \lambda e^{\lambda t} w. \end{aligned} \tag{4.14}$$

The *typical* situation for a matrix $\mathbf{A}$ of size $k \times k$ is that it will have have k distinct eigenvalues and corresponding eigenvectors. Then the general solution to $\dot{x} = \mathbf{A}x$ is a sum of exponential solutions:

$$x(t) = c_1 e^{\lambda_1 t} w_1 + c_2 e^{\lambda_2 t} w_2 + \cdots + c_k e^{\lambda_k t} w_k. \tag{4.15}$$

The fact that (4.15) is a solution can be verified directly:

$$\begin{aligned}\dot{x}(t) &= c_1\lambda_1 e^{\lambda_1 t}w_1 + \cdots + \lambda_k c_k e^{\lambda_k t}w_k \\ &= c_1 e^{\lambda_1 t}\lambda_1 w_1 + \cdots + c_k e^{\lambda_k t}\lambda_k w_k \\ &= c_1 e^{\lambda_1 t}\mathbf{A}w_1 + \cdots + c_k e^{\lambda_k t}\mathbf{A}w_k \\ &= \mathbf{A}\left(c_1 e^{\lambda_1 t}w_1 + \cdots + c_k e^{\lambda_k t}w_k\right) \\ &= \mathbf{A}x(t)\end{aligned} \tag{4.16}$$

But for the stability of a fixed point (which is at $x = 0$ for linear systems) only one term in the sum really matters.

- **Example:** $x(t) = c_1 e^{2t}w_1 + c_2 e^{-3t}w_2$. The e^{-3t} term doesn't matter in the long run, since it goes to 0.
- **Example:** $x(t) = c_1 e^{2t}w_1 + c_2 e^{t}w_2$. The e^{t} terms doesn't matter in the long run, since the other term grows much faster ($e^t/e^{2t} \to 0$).

What if there are complex eigenvalues, $\lambda = \alpha + i\omega$? The general solution (4.15) still applies, but we need to work out its implications.

$$e^{\lambda t} = e^{\alpha t}e^{i\omega t} = e^{\alpha t}(\cos(\omega t) + i\sin(\omega t)) \tag{4.17}$$

The $(\cos + i\sin)$ term always has magnitude 1 (it rotates around the unit circle in the complex plane with period $2\pi/\omega$). Therefore the magnitude of $e^{\lambda t}$ is $e^{\alpha t}$, and the change in magnitude over time is accompanied by sinusoidal oscillations.

The conclusion is that *local stability of a fixed point for a system of differential equations depends on the eigenvalue of the Jacobian with largest real part:*

- Stable if all eigenvalues of the Jacobian have negative real part.
- Unstable if any eigenvalues of the Jacobian have positive real part.
- If the largest real part of any eigenvalue is exactly 0, the equilibrium could either be stable or unstable – local linearization is inconclusive.

To reach this conclusion we have been assuming that the eigenvalues of the Jacobian are distinct, but the same holds for a Jacobian with non-distinct eigenvalues (this can be proved using Jordan Canonical form, if you've had an abstract linear algebra class).

4.3.1 The 2 × 2 case

There is a useful formula for the eigenvalues of a 2×2 matrix $\mathbf{A}$. If T is the **trace** (sum of diagonal elements) and Δ is the **determinant** ($\mathbf{A}[1,1]\mathbf{A}[2,2] - \mathbf{A}[1,2]\mathbf{A}[2,1]$) then the eigenvalues are

$$\lambda_{1,2} = \frac{1}{2}\left(T \pm \sqrt{T^2 - 4\Delta}\right) \tag{4.18}$$

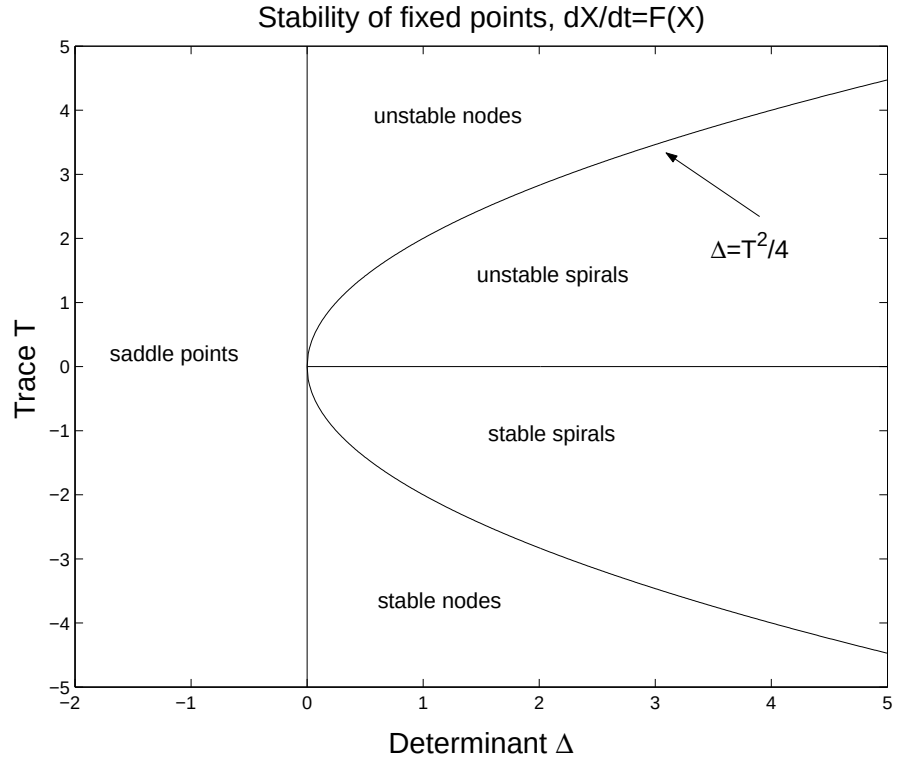

Figure 4.3: Stability analysis of 2-variable system $\dot{x} = F(x)$ in terms of the determinant D and trace T of the Jacobian matrix $\mathbf{J}$ at an equilibrium. At nodes and saddle points there are two real eigenvalues and therefore two eigenvectors; the equilibrium is a node if both eigenvalues have the same sign (negative or positive) and a saddle if they have opposite signs. At spirals the eigenvalues are complex conjugates, and solutions rotate.

This makes it possible to do a complete local stability analysis of two-dimensional differential equation systems in terms of the T and Δ (Figure 4.3). In consequence we obtain a simple criterion for local stability in the 2×2 case. In order for all eigenvalues of the Jacobian to have negative real part, we must have

$$\Delta > 0, T < 0. \tag{4.19}$$

The qualitative behavior of trajectories is also determined by the local analysis (see Figure 4.4). That Figure shows solution trajectories for the linear system. However, the Hartman-Grobman Theorem guarantees us that locally – within some small distance of the fixed point – solutions of the nonlinear system are qualitatively the same as those of the linear system, so long as none of the eigenvalues of the Jacobian has exactly zero real part.[1]

[1] A fixed points with this property is called *hyperbolic*. The precise meaning of "qualitatively the same" in the Hartman-Grobman Theorem is that the solution curves of the nonlinear system are the image of those for the linear system under some invertible continuous mapping.

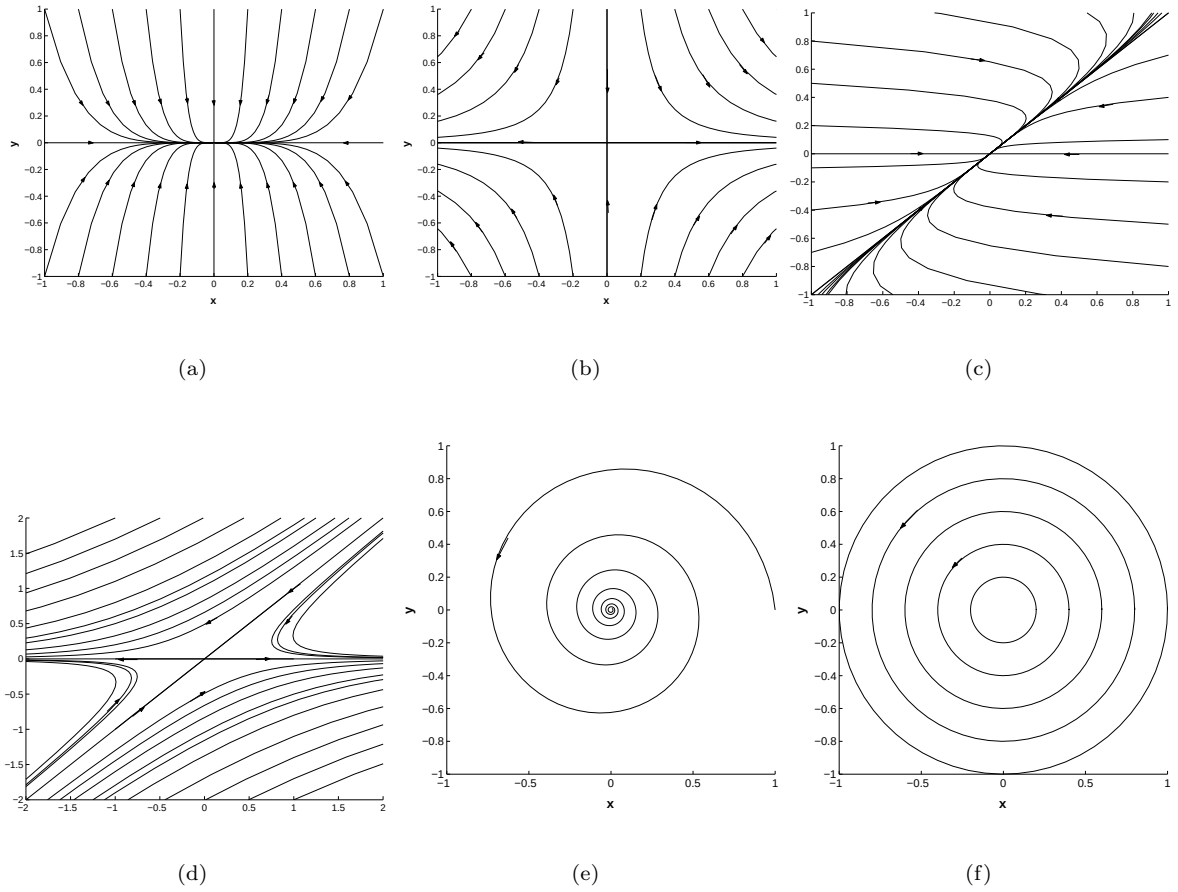

Figure 4.4: Phase portraits of two dimensional linear vector fields with a stable node (a and c) and a saddle (b and d). In (a) and (b) the eigenvectors are the coordinate axes, and in (c) and (d) the eigenvectors are not perpendicular. Panels (e) shows a stable spiral, and (f) a neutrally stable spiral where the real part of the eigenvalues is 0. An unstable node looks like a stable node, and an unstable spiral like a stable spiral, except that the arrows indicating the direction of flow point in the opposite direction. Figures provided by John Guckenheimer and incorporated without permission.

Example: The linear system $\dot{x} = \mathbf{A}x, \quad \mathbf{A} = \begin{bmatrix} -2 & 1 \\ 1 & -2 \end{bmatrix}$. To determine the behavior of solutions we can

- Write out system: $\dot{x}_1 =, \quad \dot{x}_2 =$.
- Find the eigenvalues using (4.18).
- Find the eigenvectors directly from $\mathbf{A}w_i = \lambda_i w_i$
- Plot eigenvectors and infer "phase portrait" (shape of solution curves)

Example: The Lotka Volterra system

$$\begin{aligned} \dot{n}_1 &= n_1(3 - 2n_1 - n_2) \\ \dot{n}_2 &= n_2(5 - n_1 - 4n_2) \end{aligned} \tag{4.20}$$

has interior fixed point $n_1 = n_2 = 1$. To determine stability we

- Write out f_1, f_2.
- Derive the general form of the Jacobian matrix.
- Evaluate the Jacobian at the fixed point $(1, 1)$.
- Compute the determinant and trace.
- Determine local stability from Figure (4.3).

Exercise 4.7 Use local stability analysis to verify the conclusions shown in Figure 3.3 (a) and (d) of Bulmer Chapter 3, for the stability of the interior equilibrium for the Lotka-Volterra competition equations. Note that Bulmer gives you a formula for the fixed point (equation 2, p. 31). So your tasks are to
(a) Compute the Jacobian matrix for the Lotka-Volterra model, in Bulmer's notation
(b) Evaluate the Jacobian at the interior fixed point with 3.3(a) parameters and show that the equilibrium is stable.
(c) Ditto with 3.3(d) parameters, and show that it is unstable.

Exercise 4.8 The following is a modified Lotka-Volterra model for two species interacting mutualistically

$$\begin{aligned} \dot{x} &= rx(1 - \frac{x}{K + ay}) \\ \dot{y} &= ry(1 - \frac{y}{K + bx}) \end{aligned} \tag{4.21}$$

(a) Show that if $ab < 1$ this model has an equilibrium $(\hat{x}, \hat{y})$ with $\hat{x} > 0$ and $\hat{y} > 0$. **(b)** Is the positive equilibrium from part (a) stable or unstable?
(c) Your conclusions in (a) and (b) did not depend on the values of r or K (if you got the right answers). Why?

Exercise 4.9 In this exercise, local stability analysis will be used to conjecture the global behavior of a "resource competition" model with one species present:

$$\begin{aligned} \dot{R} &= \delta(R_0 - R) - N\frac{VR}{K + R} \\ \dot{N} &= \chi N\frac{VR}{K + R} - \delta N \end{aligned} \tag{4.22}$$

with R_0, V, K, χ, δ positive constants. This represents a flow-through system (e.g. a pond or laboratory mesocosm with equal inflow and outflow) with δ being the flow rate (e.g., if 10% of the pond water is lost

to outflow each day and replaced by inflowing stream water, then $\delta = 0.1/d$). $\frac{VR}{K+R}$ is the per-individual rate at which organisms (N) take up the limiting nutrient (R), and χ is the conversion rate between nutrient uptake and birth rate.

(a) Show how the model can be re-scaled to dimensionless form

$$\begin{aligned} \dot{r} &= r_0 - r - x\frac{r}{1+r} \\ \dot{x} &= \varepsilon x \frac{r}{1+r} - x \end{aligned} \tag{4.23}$$

and give the expressions for its state variables (r, x) and parameters (r_0, ε) in terms of those of the original model.

(b) Show that there is always an equilibrium with $\hat{x} = 0$; what does this correspond to biologically [hint: this is easy].

(c) Use local stability analysis to find the conditions on parameters under which this first equilibrium is locally stable versus unstable.

(d) Show that for some (but not all) values of the parameters, there is a second equilibrium with $\hat{x} > 0$; in particular find this second equilibrium and the conditions under which it exists with $\hat{x} > 0$.

(e) Use local stability analysis to find the conditions on parameters under which this second equilibrium is locally stable versus unstable.

(f) Identify the type of the second equilibrium on the basis of Figure (4.3), as a function of parameter values (i.e. what possible types can it be, and for which range of parameters does each occur?).

(g) Put these pieces together to make a reasonable guess about what happens in general in this system, for different possible values of the parameters. That is: imagine an experiment in which the system is started at some values of $R(0), N(0)$ with $N(0) > 0$. What are the possible long-term outcomes, for which different values of the parameters?

4.4 Predator-prey interactions: functional response and the paradox of enrichment

The classic model for predator-prey dynamics is again the Lotka-Volterra model,

$$\begin{aligned} \dot{n}_1 &= r_1 n_1 - \alpha_1 n_1 n_2 \\ \dot{n}_2 &= \alpha_2 n_1 n_2 - r_2 n_2 \end{aligned} \tag{4.24}$$

This was proposed as a minimal model for fish stocks in the Adriatic. A fisheries biologist, Umberto D'Ancona, compared catch statistics before, during and after the first World War. Fishing in the Adriatic dropped nearly to nil during the war. D'Ancona observed that predatory fish (which feed on other fish) became more common during the War, relative to the periods just before and after the war. Prey fish species showed the reverse pattern. D'Ancona knew who to ask for an explanation: his father-in-law

Vita Volterra, who was (and remains – or at least his remains remain) a famous mathematician. Volterra developed the model (4.24) and showed that it could explain D'Ancona's observations (Volterra 1926).

Model (4.24) also makes some untenable predictions. In particular, the positive equilibrium is a neutrally stable center surrounded by a family of neutrally stable periodic orbits, qualitatively like the neutrally stable center of a linear system in Figure 4.4. Fortunately these go away when the model is made more realistic. The classic general form for an unstructured predator-prey model is

$$\begin{aligned} \dot{x} &= f(x) - yg(x) \\ \dot{y} &= eyg(x) - \mu y \end{aligned} \tag{4.25}$$

The change in the numbers of prey x is a balance between intrinsic births and deaths at net rate $f(x)$, and predation with $g(x)$ being the per-predator rate of prey capture. Predator y change is a balance between births (with breeding proportional to eating) and natural mortality. It would typically be assumed that f is logistic-like, so that prey in the absence of predators would reach a steady-state limited by their resource supply. Until very recently the assumption in (4.25) that g only depends on x was nearly universal – each predator in the model responds independently to the density of prey and is unaffected by other predators. The function $g(x)$ would be taken as monotonically increasing, and saturating. Typical forms are shown in Figure 4.5.

The classical form (4.25) obscures a crucial feature of any consumer-resource model – the prey and predator birth rates are *both* proportional to the *prey* abundance, when breeding is proportional to eating. To see why this holds, we need a different parsing of the terms in (4.25). The predator net birth rate $f(x)$ can be broken down as

$$f(x) = (\#\text{ prey}) \times (\text{prey per capita birth-death rate}) = x \times \frac{f(x)}{x}. \tag{4.26}$$

The capture rate $yg(x)$ can be broken down as

$$(\#\text{ prey}) \times (\text{probability of capture per unit time}) = x \times \frac{yg(x)}{x} \tag{4.27}$$

and the predator birth rate is the same multiplied by the conversion efficiency e. So $g(x)/x$ is the probability per unit time that any one given prey individual will be captured and consumed by any one given predator.

Model (4.25) is bare-bones at best, but it's a place to start. Making it more realistic might involve

- a time delay between eating and producing new offspring (Harrison 1995, Jost and Ellner 2000).
- mechanistic prey dynamics rather than a logistic-type equation.
- predator self-limitation.
- predator interference, replacing $g(x)$ with $g(x, y)$ that is a decreasing function of y.

The last of these is potentially the most important omission from the basic model. Recent studies suggest that in many cases – perhaps even most – the rate of consumption by each predator is a decreasing

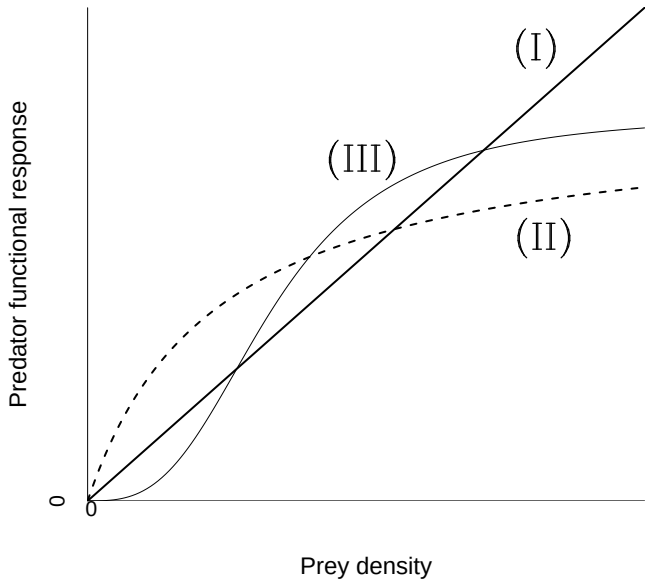

Figure 4.5: Predator functional response functions $g(x)$. The linear, saturating, and sigmoid forms are referred to as type I, II, and III respectively.

function of predator density, all else being equal. This has been found even in systems such as microbial microcosms where it is not at all clear how interference might occur (Skalski-Gilliam, Ginzburg-Abrams, Jost-Ellner).

Example: The *Rosenzweig-MacArthur model* uses logistic f and a type-II g. Note that type-II is the consumption rate equation we derived long ago (the prey model of optimal foraging theory) for a consumer hunting for a single kind of resource.

For analysis we consider the generic model (4.25) without predator interference. The typical qualitative shapes of the rate functions are shown in Figure 4.6. As usual we start by looking for steady states, via the nullclines. We have $\dot{y} = 0$ when $g(x) = \mu/e$ so the predator nullcline is the line

$$x = x^* \equiv g^{-1}(\mu/e). \tag{4.28}$$

The prey nullcline is the curve

$$y = f(x)/g(x) \tag{4.29}$$

which is well-defined except possibly at $x = 0$, depending on how f and g behave at the origin.

Do the nullclines intersect in the first quadrant – are there any equilibria? The predator nullcline is a vertical line at $x = x^*$. The prey nullcline is a curve that is positive for $x < K$ and negative for $x > K$. The nullclines therefore intersect in the first quadrant if and only if $x^* < K$. This condition can be interpreted biologically. K is the density that the prey will reach on their own, with predators

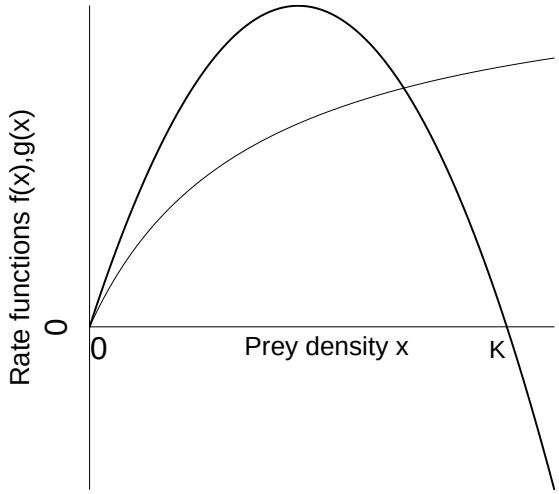

Figure 4.6: Rate functions for the basic predator-prey model. The bold curve is prey self-limitation $f(x)$, the light curve is the predator functional response $g(x)$. Though f is not necessarily logistic, we use K to denote the prey density at which f goes from positive to negative, representing a stable equilibrium for the prey in the absence of predators.

absent. x^* is the prey density at which predator births and deaths balance exactly – any lower and the predator population declines. So the relative values of x^* and K determine whether or not a few rare predators could increase, if they were introduced into a population of prey at steady state. If so, there's a steady state (x^*, y^*) with both prey and predators present at positive density. If not, then the only steady states are $(0, 0)$ and $(K, 0)$. And since the prey can never get above K (having predators around only makes things worse), the predators must decline and go to extinction. So in order for the prey and predators to coexist we must assume that $x^* > K$, and the prey and predator nullclines intersect at the steady state

$$x^* = g^{-1}(\mu/e), \quad y^* = f(x^*)/g(x^*) = ef(x^*)/\mu. \tag{4.30}$$

To determine the stability of the steady state we compute the Jacobian matrix of (4.25),

$$J = \begin{bmatrix} f'(x) - yg'(x) & -g(x) \\ eg'(x)y & eg(x) - \mu \end{bmatrix}. \tag{4.31}$$

At the steady state (x^*, y^*) this becomes

$$J^* = \begin{bmatrix} f'(x^*) - y^*g'(x^*) & -\mu/e \\ eg'(x^*)y^* & 0 \end{bmatrix}. \tag{4.32}$$

We therefore have determinant and trace

$$\begin{aligned} \Delta &= \mu g'(x^*)y^* > 0 \\ T &= f'(x^*) - y^* g'(x^*) \end{aligned} \tag{4.33}$$

The trace is positive (implying instability of the fixed point) if

$$f'(x^*) > y^* g'(x^*);$$

what does that mean? Since $y^* = y^* = f(x^*)/g(x^*)$, at (x^*, y^*) we have

$$\begin{aligned} T = f' - \frac{f}{g}g' = \frac{f'g - g'f}{g} &= g\left(\frac{f'g - g'f}{g^2}\right) \\ &= g \times \frac{d}{dx}\left(\frac{f}{g}\right) \end{aligned} \tag{4.34}$$

and $y = f(x)/g(x)$ is the prey nullcline. So *the trace has the same sign as the slope of the prey nullcline*, and the steady state undergoes a Hopf bifurcation whenever (as parameters change) the slope of the prey nullcline goes from negative to positive.

The behavior of f/g therefore determines whether the steady state is stable or unstable. We know f/g goes from positive when x is small to negative when $x > K$ – the question is: how does it get there? If f/g goes down monotonically, the steady state is always stable. If it isn't monotonic we have the potential for cycles.

Cycling versus stability therefore depends crucially on the form of the predator functional response. With a type-I functional response (Figure 4.5) $g(x) = ax$, the prey nullcline is proportional to $f(x)/x$, which is the per-capita growth rate of the prey. In order to have cycles, this must have a maximum at some intermediate value of x, rather than decreasing monotonically at higher prey density. That is, there has to be an Allee effect in the prey, otherwise the fixed point is always stable.

With a type-II functional response the prey nullcline can have a hump even without an Allee effect in the prey. For this reason it is often said that "a type-II functional response is destabilizing". For example, consider the Rosenzweig-MacArthur model

$$\begin{aligned} f(x) &= rx(1 - x/K) \\ g(x) &= ax/(1 + bx) \end{aligned}$$

for which the prey nullcline is

$$\frac{f(x)}{g(x)} = \frac{rx(1 - x/K)(1 + bx)}{ax} \propto (1 + bx)\left(1 - \frac{x}{K}\right). \tag{4.35}$$

The prey nullcline will have a hump if its derivative at $x = 0$ is positive. This will be proportional to the derivative at 0 of the last expression in (4.35), which is $b - \frac{1}{K}$. The prey nullcline therefore has a hump (and cycles are possible) if $bK > 1$. If bK there is no hump and the fixed point is stable. A bit of calculus shows that the hump in the prey nullcline is at

$$x_h = \frac{bK - 1}{2b}. \tag{4.36}$$

So an increase in K moves the hump in the prey nullcline further and further to the right. However, it has no effect on the predator nullcline, which remains at $x^* = g^{-1}(\mu/e)$ So if K keeps increasing, eventually $x_h > x^*$ and the fixed point goes from unstable to stable via a Hopf bifurcation. This behavior is known as the *paradox of enrichment*. Enrichment of the system's resource base – reflected in a higher prey carrying capacity – is beneficial up to a point, but eventually it destabilizes the system.

Another interpretation of this result is that it predicts a *suppression-stability* tradeoff (Murdoch et al. 2003): cycles occur if $K \gg x^*$. That is, if the level to which the predator can suppress the prey (at steady state) is far below the intrinsic carrying capacity of the prey, then cycles are predicted. This prediction is especially interesting because there are many striking counterexamples: natural populations that are held stably by predators at numbers far lower than they can reach when predators are absent (Murdoch et al. 2003). It also has the interesting interpretation that *biological control of pest species should be impossible:* any control agent that can reduce pest numbers appreciably should be unable to do so permanently, instead there should be periodic outbreaks of the pest. Biological control has had mixed success, and perhaps this is one reason for it – but biological control has also had some successes, which are therefore hard to explain. We'll come back to this later in this chapter.

The form of the Jacobian (4.31) explains why consumer-resource interactions and other exploiter-victim interactions are generally prone to cycle. The nature of the interaction means that the resource abundance has a strong positive impact on the consumer, while the consumer abundance has a strong negative impact on the resource species. We therefore get Jacobians of the form

$$J = \begin{bmatrix} r & + \\ - & c \end{bmatrix} \tag{4.37}$$

where r and c represent the self-regulatory effects of resource and consumer species density on their own species' growth. If the within-species effects are weak compared to the trophic interaction, we have

$$\begin{aligned} \Delta &= (\text{small})(\text{small}) - (+)(-) > 0 \\ T &= \text{ small} + \text{small } \approx 0 \end{aligned} \tag{4.38}$$

A fixed point for the system is therefore sitting near the boundary between stable and unstable spirals – that is, between damped and undamped oscillations around the fixed point. Even if the fixed point is stable, random perturbations (weather, accidents of demography in finite populations, and so on) will continually kick it away from the fixed point, so the observed dynamics would often be somewhat cyclic.

Exercise 4.10 Here is a more general consideration of how a type-II functional response is destabilizing relative to a type-I. As we noted above, the prey nullcline must have a hump if the curve $y = f(x)/g(x)$ has positive slope at $x = 0$. Show that if $g'(0) > 0$ this slope has the same sign as

$$g'(0)f''(0) - f'(0)g''(0).$$

(Note: this will require two applications of L'Hopital's rule to resolve 0/0 limits.) So all else being equal, a negative second derivative in the predator functional response g will tend to increase the slope at 0 and favor a hump in the prey nullcline.

Exercise 4.11 What happens with a type-III (accelerating) functional response by the predator – Is it stabilizing or destabilizing relative to a type-I (linear) functional response? A typical type-III response equation would be $g(x) = ax^2/(1+bx^2)$, where x is the prey density. This eventually saturates for large x, and before that starts looking like a type-II (concave down rather than up). So to see what can be "new and different" in type-III, for this exercise consider instead $g(x) = ax^2$.

4.5 Discrete time models

4.5.1 Nicholson-Bailey model

The prime example of an ecologically interesting discrete-time model for interacting populations is the Nicholson-Bailey model for host-parasitoid dynamics. Parasitoids are insect species (some terrestrial, some extraterrestrial as in the *Aliens* movies) whose larvae develop by feeding on the bodies of other arthropods, usually killing them. Larvae emerge from the host and develop into free-living adults. The adults then lay their eggs in a subsequent generation of hosts. Most parasitoid larvae require a specific life-stage of the host, so parasitoid and host generations are linked to one another. Consequently host-parasitoid models often use a discrete time step corresponding to the common generation length of host and parasitoid.

Every important idea in theoretical ecology has been applied to the study of host-parasitoid dynamics, for two main reasons:

- Practical importance. Biological control of insect pests – as a part of integrated pest management aimed at reducing chemical pesticide use – is largely through introduction of parasitoids. The goal is to produce low, stable numbers of the pest.
- Theoretical interest. There are a lot of things about real host-parasitoid systems that simple models cannot explain. So it becomes an arena for adding all sorts of complications - spatial dynamics, metapopulations, stage structure, foraging theory - to see what can happen.

The classic model was derived by Nicholson and Bailey (1935). There were hoping to publish a book on the subject, but their proposal was rejected due to the expectation that ecologists would not be interested in a book full of equations. Nicholson and Bailey's only real problem was being 30 years ahead of their time, and ecology might be a very different field today had their book been published. The assumptions of the Nicholson-Bailey model are as follows:

- Hosts are distributed at random, at density H_t per unit area in generation t
- Parasitoids search at random and independently, each having an "area of discovery" a, and lay an egg in each host found.
- Each parasitized host gives rise to 1 new parasitoid in generation $t+1$
- Each unparasitized host gives rise to $R > 1$ new hosts in generation $t+1$

Each parasitoid attacks the hosts found in a units of area, so the expected number of hosts attacked is by each parasitoid is aH. The expected total number of attacks is aPH. The total number of attacks can also be written as the sum over hosts of the number of attacks on each host. All hosts have the same expected number of attacks, so the expected number of attacks on any given host must be aP. Under the assumptions listed above, the number of eggs per host has a Poisson distribution (see the Appendix at the end of this chapter). Consequently, the expected fraction of hosts that are not parasitized is the probability that a Poisson random variable with mean aP takes the value zero, which $e^(- aP)$. The resulting population dynamics are

$$\begin{aligned} H_{t+1} &= RH_t e^{-aP_t} \\ P_{t+1} &= H_t \left(1 - e^{-aP_t}\right) \end{aligned} \tag{4.39}$$

4.5.2 Local stability analysis

To see how the Nicholson-Bailey model behaves, we (once again) start by finding fixed points and analyzing their stability. Consider a general multispecies difference equation model

$$n_i(t+1) = F_i(n_1(t), n_2(t), \cdots, n_k(t)), i = 1, 2, \cdots, k \tag{4.40}$$

which we can write compactly as

$$n(t+1) = F(n(t)). \tag{4.41}$$

A fixed point of the model is then a solution of

$$\hat{n} = F(\hat{n}). \tag{4.42}$$

To study the dynamics near a fixed point we (once again) use linearization. Writing $p(t) = n(t) - \hat{n}$ and proceeding as we did above for a differential equation model, the local dynamics are approximated by

$$p(t+1) = \mathbf{J}p(t) \tag{4.43}$$

where $\mathbf{J}$ is again the Jacobian matrix for F evaluated at the fixed point, i.e. the $(i,j)^{th}$ element of $\mathbf{J}$ is $\frac{\partial F_i}{\partial n_j}$ evaluated at $\hat{n}$. In the *typical* case where the eigenvalues are all distinct, the general solution to (4.43) will (once again) be a sum of exponential terms, but these are not quite the same as for a differential equation model:

$$p(t) = c_1\lambda_1^t w_1 + c_2\lambda_2^t w_2 + \cdots + c_k\lambda_k^t w_k. \tag{4.44}$$

The conclusion from (4.44) is that the fixed point is locally stable if all eigenvalues of the Jacobian are less than 1 in absolute value, and is locally unstable if any eigenvalues are greater than 1 in absolute value – recall that for for a complex eigenvalue $\lambda = a + ib$ the absolute value is

$$|\lambda| = \sqrt{a^2 + b^2}. \tag{4.45}$$

As for differential equation models, the local stability criterion also applies when there are repeated eigenvalues.

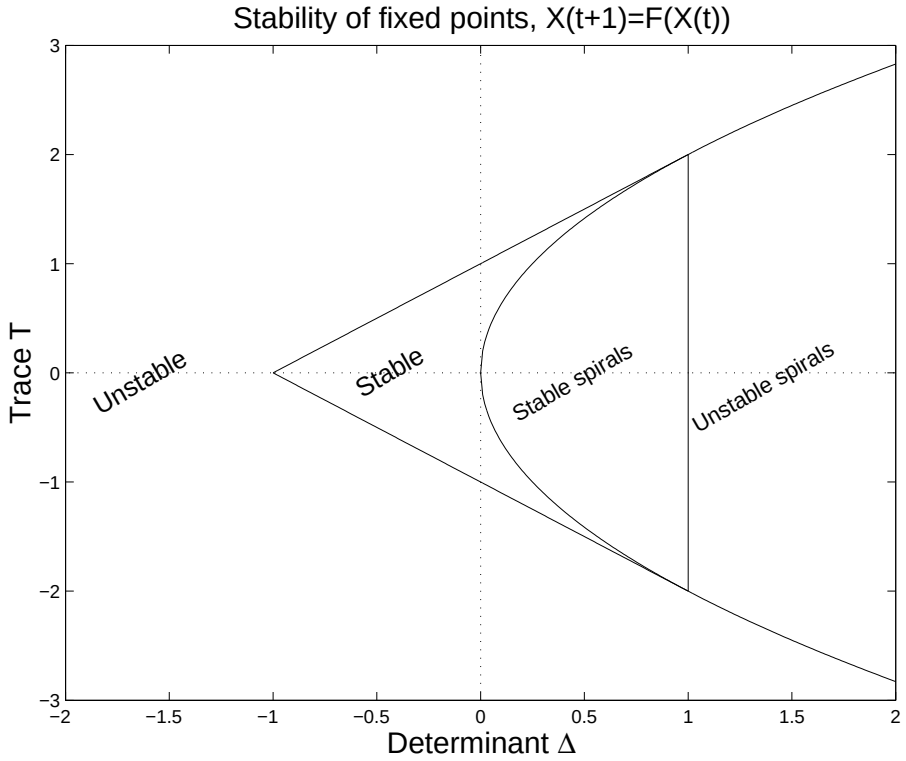

Figure 4.7: Stability analysis of 2-variable system $X_{t+1} = F(X_t)$ in terms of the determinant Δ and trace T of the Jacobian matrix $\mathbf{J}$ at an equilibrium. At spirals the eigenvalues are complex conjugates, and solutions rotate. Otherwise both eigenvalues are real; if $\Delta > 0$ they have the same sign (equal to that of the Trace), and if $\Delta < 0$ they have opposite signs.

For 2×2 systems we still have the eigenvalue formula

$$\lambda_{1,2} = \frac{1}{2}\left(T \pm \sqrt{T^2 - 4\Delta}\right) \tag{4.46}$$

where T is the trace and Δ the determinant of the Jacobian matrix at a fixed point. Using this, the condition for local stability of a fixed point (both eigenvalues < 1 in absolute value) is

$$|T| < 1 + \Delta < 2 \tag{4.47}$$

The curve $\Delta = T^2/4$ separates real versus complex eigenvalues, so as in the continuous time-case we get spirals when $4\Delta > T^2$. These results are summarized in Figure 4.7.

4.5.3 Analysis of Nicholson-Bailey

First we need to find steady states $(\hat{H}, \hat{P})$. The host equation gives use

$$\hat{H} = R\hat{H}e^{-a\hat{P}} \Rightarrow Re^{-a\hat{P}} = 1 \Rightarrow \hat{P} = \log(R)/a. \tag{4.48}$$

Then since $e^{-a\hat{P}} = 1/R$ the parasitoid equation gives

$$\hat{H} = \frac{R}{R-1}\hat{P} = \frac{R}{R-1}\log(R)/a. \tag{4.49}$$

We therefore have a positive steady state so long as $R > 1$.

Next we need the Jacobian. For the NB the component maps are

$$F_1(H,P) = RHe^{-aP} \qquad F_2(H,P) = H\left(1 - e^{-aP}\right).$$

Taking the necessary derivatives and simplifying, we find that the Jacobian at the fixed point is

$$J = \begin{bmatrix} 1 & -a\hat{H} \\ \frac{R-1}{R} & \frac{a\hat{H}}{R}. \end{bmatrix} \tag{4.50}$$

The determinant of the Jacobian is

$$\Delta = \frac{a\hat{H}}{R} + \frac{a\hat{H}(R-1)}{R} = a\hat{H} = \frac{R\log R}{R-1}. \tag{4.51}$$

A numerical plot shows that $\frac{R\log R}{R-1}$ is an increasing function of R for $R > 1$, and converges towards 1 as R decreases to 1. The fact that this quantity is always > 1 is equivalent to

$$q(r) \equiv R\log R - R + 1$$

always being positive for $R > 1$ – which is true because $q(1) = 0$ and $q'(R) = 1 + \log R - 1 > 0$ for all $R > 1$. Consequently, a fixed point of the Nicholson-Bailey model is always unstable because $1 + \Delta > 2$ whenever the fixed point exists. Numerical solutions show that the actual dynamics are highly unstable (Figure 4.8). Oscillations diverge away from the fixed point, and lead to extreme outbreaks and crashes that could not be sustained in the real world.

Exercise 4.12 Show that the eigenvalues of the Jacobian for the Nicholson-Bailey model's steady state are always complex, by showing that $T^2 - 4\Delta < 0$ for all $R > 1$.

Exercise 4.13 (a) Show how the Nicholson-Bailey model can be rescaled to eliminate the parameter a. (b) Use numerical simulation to study the behavior of the Nicholson-Bailey model for different values of R.

4.5.4 Stabilizing host-parasitoid models

The stability of actual host-parasitoid systems – contrasted with the extreme instability of the Nicholson-Bailey model – is therefore something of a mystery. As modelers we can modify the model until it stabilizes. Theoreticians have come up with a number of different modifications that can achieve stability, that fall mainly in two categories:

- Additional forms of density dependence, such as parasitoid interference (with the per-parasitoid search area a replaced by some some decreasing function of parasitoid density) or intrinsic self-limitation in the host.

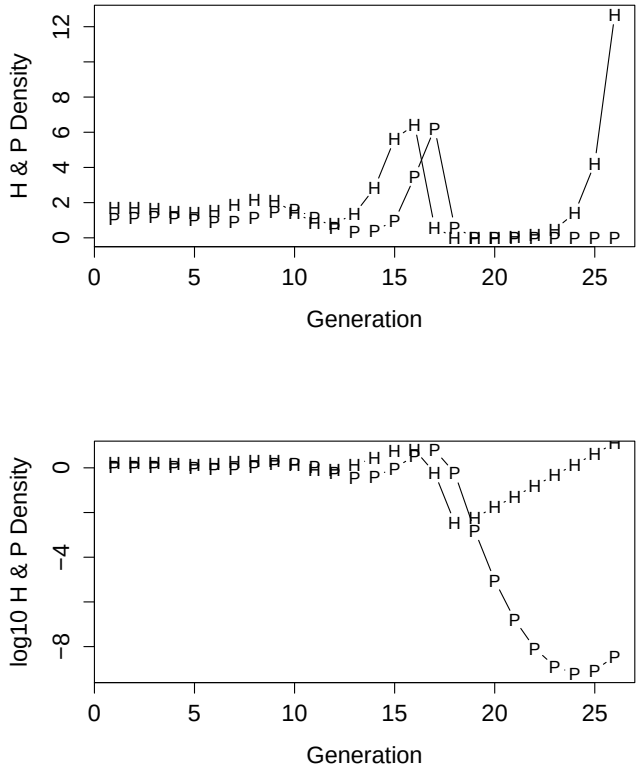

Figure 4.8: Dynamics of the Nicholson-Bailey model with $R = 3$.

- Spatial population dynamics, ranging from simple (a host refuge) to baroque (spatial chaos in systems of coupled host-parasitoid models).

The existence of theoretical solutions is not satisfying without evidence to justify the changes, and that has proved surprisingly difficult. Spatial dynamics has been the main focus of work, which began in the 1970s. May (1978) proposed a phenomenological spatial model, based on assuming that hosts are distributed evenly into a set of discrete patches, and are attacked only by the parasitoids in that patch. If parasitoids are distributed among patches independently, the Nicholson-Bailey model results. But if parasitoids aggregate (so patches tend to either have a lot of parasitoids, or just a few), more stable dynamics can result. One influential example assumed a gamma distribution for the parasitoid density in each patch, which led to a negative binomial distribution for the number of attacks per host. May (1978) showed that in that case one could write a pair of simple equations for the dynamics of the total host and parasite densities in the system of patches:

$$\begin{aligned} H_{t+1} &= RH_t(1 + aP_t/k)^{-k} \\ P_{t+1} &= H_t(1 - (1 + aP_t/k)^{-k}) \end{aligned} \tag{4.52}$$

where k is equal to the inverse of the squared coefficient of the number of parasitoids per patch, $k = 1/CV_p^2$. Note that as $k \to \infty$ this converges to the Nicholson-Bailey model (using the result from calculus that $(1 + x/n)^n \to e^x$).

Stability analysis of this model (May 1978) yielded a very simple result: the interior fixed point is stable if $k < 1$. The condition for stability is thus

$$CV_p^2 > 1. \tag{4.53}$$

This equation then proceeded to take on a life of its own. It was initially interpreted as saying that stability would ensue if parasitoids aggregate on patches with the most hosts. Eventually it was realized that **any** kind of aggregation would be stabilizing – for example, if parasitoids aggregate on patches with the fewest hosts. The key to stability in this model is that some hosts are at relatively high risk of attack, others at relatively low risk.

By the early 1990s, theoreticians had shown that the $CV_p^2 > 1$ rule applied, at least approximately, to a wide range of models. Empirical ecologists took advantage of the opportunity this created – to publish papers just by counting bugs. The punchline, unfortunately, was "sorry, try again". Reviewing 34 data sets with adequate data, Taylor (1993) found only 9 with $CV_p^2 > 1$, so as a general explanation for persistence of host-parasitoid systems it fails.

In the models considered so far space is *implicit* - the model specifies how parasitoids are distributed across patches, but not how they got there. Theoreticians also considered explicitly spatial models. For example, consider a regular rectangular lattice of patches, with Nicholson-Bailey dynamics within the patch and symmetric dispersal among neighboring patches (i=patch index, t=time):

$$\begin{aligned} H^*_{i,t} &= RH_{i,t}e^{-aP_{i,t}} \\ P^*_{i,t} &= H_t(1 - e^{aP_{i,t}}) \\ H_{i,t+1} &= (1 - \mu_H)H^*_{i,t} + \mu_H \bar{H}_{i,t} \\ P_{i,t+1} &= (1 - \mu_P)P^*_{i,t} + \mu_P \bar{P}_{i,t} \end{aligned} \tag{4.54}$$

where $\bar{H}_i, \bar{P}_i$ are the averages of H^*, P^* over the 8 patches surrounding patch i(Hassell et al. 1991, Comins et al. 1992). This model was found to exhibit coexistence either as a "crystal lattice" (an unchanging pattern of spatially varying densities, which occurs when μH is low and μ_P is high), spiral waves, or spatial chaos (Figure 4.9). In the latter two cases coexistence occurs through hosts dispersing into relatively unoccupied patches, and being consumed by a following wave of parasitoids which then dies out – but not before some hosts have moved on. Both of these mechanisms depend on the within-patch dynamics being unstable. *Local* instability generates *large-scale persistence* – host and parasite are both abundant at all times, but in different places.

Unfortunately, explicitly spatial modeling did not provide a refuge from the conflict with empirical studies. For cases where coexistence occurs in the explicitly spatial models, the resulting spatial distribution of parasitoids satisfies the condition derived in the phenomenological models: $CV_p^2 > 1$. So the empirical evidence against the phenomenological models applied equally well to explicitly spatial models – not to

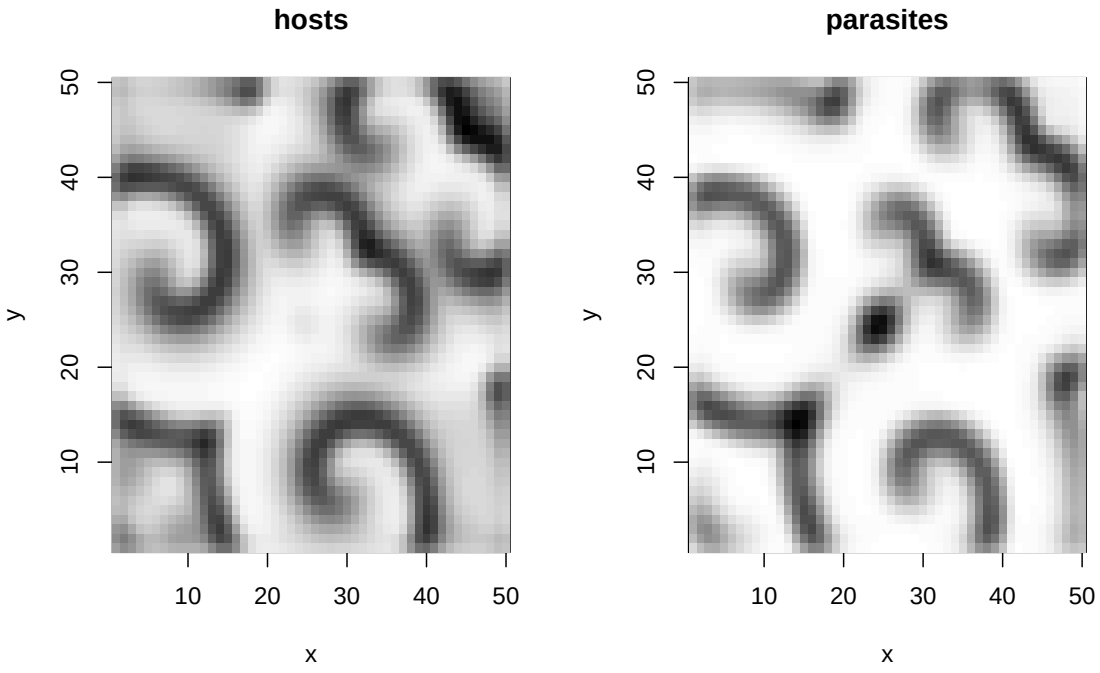

Figure 4.9: Spiral waves produced by the spatial Nicholson-Bailey model (4.54). Darkness is proportional to the square root of host and parasitoid density. This simulation had $a = 1, R = 2, \mu_H = \mu_P = 0.8$ on a 50×50 square lattice with absorbing boundaries – individuals who migrate off the lattice are lost from the population

.

mention the fact that spiral waves or spatial chaos have not yet been observed in any real host-parasitoid system (Rohani et al. 1997). Undaunted, theoreticians went on to consider 3-species systems (e.g., two parasitoids on one host) in the same kind of lattice system (Comins and Hassell 1996, with the admission that "theory is far ahead of experiment or observation").

Exercise 4.14 : (based on exercise 9 in Bulmer Ch. 3). Consider the Nicholson-Bailey model proposed by Hassell and Varley, with interference between parasitoids such that the search area per parasitoid is inversely proportional to $\sqrt{P_t}$:

$$\begin{aligned} H_{t+1} &= RH_t e^{-a\sqrt{P_t}} \\ P_{t+1} &= H_t(1 - e^{-a\sqrt{P_t}}) \end{aligned} \tag{4.55}$$

(a) Show how the model can be rescaled to eliminate a (i.e. so that the equations look just like the ones above, but with $a = 1$).
(b) Show that for $R > 1$ this model has an equilibrium $(\bar{H}, \bar{P})$ with $\bar{H} > 0, \bar{P} > 0$.
(c) Show that this internal equilibrium is stable for $R < 4.92$, by numerically evaluating and plotting the absolute value of the dominant eigenvalue of the Jacobian at $(\bar{H}, \bar{P})$ as a function of R. The ideal

solution for this problem would consist of three parts: (1) a derivation of the Jacobian matrix at $(\bar{H}, \bar{P})$, (2) a script file that evaluate the dominant eigenvalue as a function of R, and (3) a plot of results from the script file.
(d) Propose a more general version of this model, and derive a prediction about it using methods like those above. For example, your more general model will have at least one more parameter. What effect does that parameter have on existence and stability of the internal equilibrium?

Exercise 4.15 We consider here a simple discrete-time host-pathogen model for spread of an infectious disease with permanent immunity. The time-step is equal to the duration of the infectious phase. The state variables are S_t, the number of susceptible individuals at time t, and C_t representing the number of individuals getting the disease (new cases) between times $t-1$ and t.

$$\begin{aligned} C_{t+1} &= S_t(1 - e^{-\beta C_t}) \\ S_{t+1} &= S_t + B - C_{t+1} = S_t e^{-\beta C_t} + B \end{aligned} \tag{4.56}$$

Here B is the number of births between t and $t+1$, all added to the susceptible class and assumed to be constant over time. So the second line of the model is just "conservation of mass" for the Susceptible class. The first line is like Nicholson-Bailey: it comes from assuming that each susceptible escapes infection with probability $e^{-\beta C_t}$ – the more infectives there are, the lower the chance of escape. The model ignores mortality in the susceptible class, on the assumption that everyone gets the disease while young and mortality occurs later in life.
(a) Analyze this model with regard to existence and local stability of steady states, and use simulations to check your conclusions.

(b) Re-interpret the results of (a) for host-parasitoid dynamics.

(c) Generalize your analysis to the case where there is host mortality at rate $d > 0$, and the susceptible dynamics become $S_{t+1} = (1-d)S_t + B - C_t$.

4.6 Understanding stability: red scale

Murdoch (1994) reviews efforts over 15 years to understand stability of the interaction between California red scale (host) and its introduced parasitoid *Aphytis melitus*. Red scale is a citrus pest that has been successfully controlled by the parasitoid. It has been held for decades at about a 99% reduction relative to its pre-control density, and is one of the least variable insect populations on record (Murdoch 1994). There is no evidence of local extinctions and recolonizations (as occur in "spatial chaos" kinds of models): each local population seems to be stable on its own.

Over (by now) 2 decades of study, Murdoch and collaborators "tested and failed to find evidence for 8 hypotheses that might account for the system's stability" (Murdoch et al. 1994).

1. Density dependent parasitoid aggregation
2. Density independent parasitoid aggregation

3. Density dependence in the parasitism rate (e.g. parasitoid interference as in the Hassell-Varley model above)
4. Density-dependent sex ratio in the parasitoid
5. Refuge for the host: if the interior of the tree is relatively safe for hosts, some of whom could "leak" out and stabilize the exterior population in the foliage. There was a significant refuge (over 90% of reproductive female red scale were in the refuge), but in experiments where the refuge population was eliminated, the variability of the exterior population did not go up.
6. Spatial population dynamics of various sorts (no: isolating individual trees from one another did not increase the variabilty of populations).
7. Density dependence in the host (an odd hypothesis, since the host is kept at such low levels)
8. Limitation of the host by predators (also odd, since predators would be expected not to focus on such a rare species)

So what else might it be? Murdoch (1994) considered 3 other explanations based on stage structure in the two populations.

1. Adult hosts are invulnerable to attack, and this can cause stability in models, but not at realistic parameter values (stage durations) for this system
2. Size selectivity by the parasitoid: in small host individuals the parasitoid lays male eggs (or eats the host instead), in large hosts it lays female eggs. For this model, estimated parameters are very close to the stability border.
3. Cannibalism by the parasitoid (when eating small hosts that have already been parasitized). In models this is very stabilizing.

These last ideas have not yet been tested. If they do provide an explanation for red scale, it is still not an encouraging result. These mechanisms depend on the specifics of this system, and would not provide a general explanation for the persistence of host-parasitoid interactions.

The lack of a simple explanation has not decreased interest in host-parasitoid dynamics (see Hochberg and Ives 2000) but it means that theory is now dominated by more complicated models. Another important change in direction resulted from a paper by Murdoch and Stewart-Oaten (1989) that questioned the relevance the emphasis on parasitoid aggregation that started with May (1978). MSO noted that the spatial extensions of the Nicholson-Bailey framework all make the unrealistic assumption that parasitoids only move once per generation. As an opposite extreme, MSO considered a continuous-time version of the Nicholson-Bailey model where parasitoids could re-aggregate continuously across a set of patches differing in host density. They discovered that

- Aggregation of parasitoids could be stabilizing or destabilizing if it occurs in response to host density; if it is independent of host density it has no effect at all.

- Stability is not affected by the degree of host patchiness *per se* but on how it varies in response to mean host density.

This says that any static measure of spatial variability such as CV_p^2 are irrelevant. What matters for stability is how they are generated – the response of parasitoids and hosts to variation in host density. On the other hand, the assumption of instantaneous redistribution by omniscient parasitoids in response to host density is no more realistic than the alternative of one-per-generation redistribution. As a result, current models tend to be burdened with many details of host and parasitoid life-cycles, dispersal behavior and foraging behavior.

Exercise 4.16 This and the following exercises develop the model of Murdoch and Stewart-Oaten (1989) for a host-parasitoid system with continuous attack rather than discrete generations, and continuous redistribution of parasitoids based on host density. For a single patch, the Nicholson-Bailey model becomes

$$\frac{dH}{dt} = aH - bHP \qquad dPdt = cHP - dP. \tag{4.57}$$

This is a Lotka-Volterra predator-prey model, whose fixed point (when it exists) is always neutrally stable. Now consider a multi-patch system with h and p denoting the average densities of hosts and parasitoids across patches. Show that

$$\frac{dh}{dt} = ah - b(hp + Cov(H,P)) \qquad dpdt = c(hp + Cov(H,P)) - dp \tag{4.58}$$

where $Cov(H,P) = E(HP) - E(H)E(P)$ and E denotes the average across patches. This shows that, in contrast to models with once-per-generation movement, parasitoid aggregation that is independent of host density (hence $Cov(H,P) = 0$) has no effect on stability – the spatial system is then identical to the one-patch system.

Exercise 4.17 To go further we need an expression for $Cov(H,P)$ in terms of h and p. To get that, Murdoch and Stewart-Oaten assume that parasitoids respond instantly and omnisciently to the distribution of hosts such that $E(P_i|H_i) = p(1 + G(H_i,h)$ where the subscript i indicates densities in patch i. They also assume that the distribution of hosts across patches depends only on the mean density h (e.g., a Poisson distribution). This gives

$$E(HP) = E(Hp(1 + G(H,h)) = hp + pE(HG(H,h)) = hp + pQ(h) \tag{4.59}$$

where $Q(h) = E(HG(H,h))$ – this implies $Cov(H,P) = pQ(h)$. The spatial model is then

$$\frac{dh}{dt} = ah - bp(h + Q(h)) \qquad dpdt = cp(h + Q(h)) - dp. \tag{4.60}$$

Suppose that a nonzero steady state $(\hat{h}, \hat{p})$ is locally stable if $Q'(\hat{h}) > Q(\hat{h})/\hat{h}$ and locally unstable if the reverse inequality holds. Interpret this condition in terms of the shape of $Q(h)$ and of the predator functional response $g(h) = h + Q(h)$ (note that the condition for stability is equivalent to $g'(\hat{h}) > g(\hat{h})/\hat{h}$).

Exercise 4.18 Suppose that there is density-dependent parasitoid aggregation, with a linear response to relative host density: $G(H,h) = m(H-h)/h$ where m is a constant. Suppose further that $Var(H) = Ah^x$

for $A > 0$ and some $x > 0$ – this form for the relationship between the mean and variance of density across habitat patches is called *Taylor's power law*. Show that the steady state may be either stable or unstable, depending on the value of x. The conclusion is that if parasitoids redistribute continuously in response to host density, density-dependent parasitoid aggregation can either be stabilizing or destabilizing.

4.7 Understanding cycles: larch budmoth

To end on a more upbeat note, we echo the theme of Zimmer (1999): the unreasonable *quantitative* success of relatively simple nonlinear models that 25 years ago would have been defended as "metaphors" for real ecological systems and tools for exploring ideas. As a case in point we consider the population cycles of larch budmoth, based on work of Turchin and collaborators (Turchin et al. 2002, 2003; Turchin 2003).

The larch budmoth is a classic population cycle. Budmoth density varies by nearly 5 orders of magnitude, with remarkably constant period and amplitude (the data are graphed in the previous chapter). For the last few decades, the predominant explanation (and consequently the focus of ongoing research) has been the interaction between budmoth and its food supply, larch needles. The cycle is interpreted as a consumer-resource interaction with budmoth the consumer and larch needles the resouce. Outbreaks of budmoth leave the trees shorn of high-quality needles, and lacking the resources to produce high quality foliage the next year. The needles are then shorter and have a higher raw fiber content. Feeding on such needles results in lower larval survival and female fecundity. It takes several years for the quality of foliage to recover.

Models based on the budmoth–tree interaction can generate cycles that resemble those observed, but analysis of time-series data on budworm and needles revealed a serious discrepancy between models and data. In model solutions there is a strong reciprocal influence between budmoth density and needle quality, each affecting the other's changes. In the data one only sees a one-way effect – budmoth have a large impact on the needles, but not vice-versa. In addition, a recent outbreak (early 1990s) never reached levels at which defoliation occurred. Foliage quality remained high but the outbreak collapsed nonetheless. This indicates that foliage quality is not causal, but "along for the ride" as budmoth fluctuates for some other reason(s).

The other potential mechanism known to be operating in this system was attack by parasitoids. The parasitism attack rate can be quite high (up to 80-90%), but this mechanism had been rejected based on the timing of peak attacks. Maximal parasitism rates occur 2 to 3 years after the peaks of budmoth density, and it was argued that if parasitoids cannot even limit budmoth increase, they were are unlikely to play an important role in the decrease phase of the cycle. However this was strictly a verbal argument and proved to be flawed. In a model having both direct density dependence (e.g. a finite food supply for budnoth that sets a limit to growth) and parasitoids, the host-parasitoid interaction can generate cycles that match the observed lag between the peaks in budmoth density and parasitoid attack (Turchin et al. 2002, 2003). In fact a simple model based on the Nicholson-Bailey framework was able to account for

83% of the variance in budworm numbers, compared to only 44% explained by the best-fitting model for the budworm-foliage interaction. A more careful statistical analysis (Turchin et al. in press) showed that the budworm-foliage interaction does play a role in the cycle: although the goodness of fit to the data is only marginally improved by including that interaction, the improvement is statistically significant.

The importance of parasitoids is supported by subsequent work on the spatial dynamics of budworm outbreaks by Bj**o**rnstad et al 2002. Budworm outbreaks across Europe form a spatial "wave" moving at about 210km per year from southwest to northeast. A spatial extension of the Turchin et al (2003) host-parasitoid model, along the lines of (4.54), was able to reproduce the spatial wave under certain assumptions about moth dispersal and the spatial variation in habitat quality. However a model based on the budmoth–tree interaction was only able to produce waves travelling in the wrong direction (Bj**o**rnstad et al 2002).

The books edited by Berryman (2002) and written by Turchin (2003) review a number of other cases where quantitative modeling has been able to identify a single mechanism that is best able to account for the available data on population variability. In many cases this success depends on the availability of more information than total population counts. For example the larch budmoth data series is accompanied by less extensive data on needle length (a surrogate measure of needle quality) and the fraction of budmoth attacked by parasitoids.

So far most of the well-studied cycles seem to be driven by trophic interactions – consumer-resource, host-parasitoid, host-pathogen, or tritrophic. However in one case the most likely explanation seems to be *maternal effects*. This means that the conditions experienced by members of one generation affect the quality (and therefore the reproductive success) of their offspring. The additional state variable "individual quality" behaves much like the density of a resource species. When quality is high there is rapid population growth, but high population density brings quality down, as if it were being "consumed". As in genuinely trophic interactions, cycles are a likely outcome of population regulation by maternal effects. Analyzing and modeling data on the pine looper moth in UK forests, Kendall et al. (in press) concluded that the host-parasitoid interaction – which has been the most-studied hypothesis for the cycles in that system – is just along for the ride, while the cycles are driven by strong effects of the mother's environment on the viability of her offspring.

Because relatively few cases have been resolved, it is probably premature to generalize about the factors driving population variability. However, the ability to reach strong conclusions about well-studied systems is encouraging.

Exercise 4.19 Something about the Ginzburg-Taneyhill model for maternal effects.

4.8 References

Bj**o**rnstad, O.N., M. Peltonen, A.M. Liebhold, W. Baltensweiler. 2002. Waves of Larch Budmoth Outbreaks in the European Alps. Science 298: 1020-1023.

Comins, H.N., M.P. Hassell, and R.M. May. 1992. The spatial dynamics of host-parasitoid systems. J. Anim. Ecology 61: 735-748.

Comins, H.N. and M.P. Hassell. 1996. Persistence of multispecies host-parasitoid interactions in spatially distributed models with local dispersal. J. Theor. Biol. 183: 19-28.

Ellner, S. and P. Turchin, 1995. Chaos in a noisy world: new methods and evidence from time series analysis. American Naturalist 145: 343-375.

Hassell, M.P., J.H. Lawton, and R.M. May. 1976. Patterns of dynamical behavior in single-species populations. Journal of Animal Ecology 45: 471-486.

Hassell, M.P., H.N. Comins, and R.M. May. 1991. Spatial structure and chaos in insect population dynamics. Nature 353: 255-258.

Hastings, A. 1997. Population Biology: Concepts and Methods. Springer, NY.

Hubbell, S, S. B. Hsu and P. Waltman. 1977. A mathematical theory for single-nutrient competition in continuous cultures of micro-organisms. SIAM Journal on Applied Mathematics 32: 366-383.

Huisman, J. 1999. Population dynamics of light-limited phytoplankton: Microcosm experiments. Ecology 80:202-210.

Huisman, J., and F. J. Weissing. 1994. Light-Limited Growth and Competition for Light in Well-Mixed Aquatic Environments - an Elementary Model. Ecology 75:507-520.

Huisman, J., R. R. Jonker, C. Zonneveld, and F. J. Weissing. 1999. Competition for light between phytoplankton species: Experimental tests of mechanistic theory. Ecology 80:211-222.

Huisman, J., J. Sharples, J. M. Stroom, P. M. Visser, W. E. A. Kardinaal, J. M. H. Verspagen, and B. Sommeijer. 2004. Changes in turbulent mixing shift competition for light between phytoplankton species. Ecology 85:2960-2970.

Kendall, B.E., J. Prendergast, and O.N. Bj**o**rnstad. 1998. The macroecology of population cycles: taxonomic and biogeographic patterns in population cycles. Ecology Letters 1: 160-164.

Kendall, B.E., S.P. Ellner, E. McCauley, S.N. Wood, C.J. Briggs, W.W. Murdoch, and P. Turchin. Population cycles in the pine looper moth *Bupalus piniarius*: Dynamical tests of mechanistic hypotheses. Ecological Monographs *in press*.

Ludwig, D., D.D. Jones, and C.S. Holling. 1978. Qualitative analysis of insect outbreak systems: the spruce budworm and forest. Journal of Animal Ecology 47: 315-332.

Murdoch, W.W., B.E. Kendall, R.M. Nisbet, C.J. Briggs, E. McCauley, and R. Bolser. 2002. Single-species models for many-species food webs. Nature 417: 541-543.

Murdoch, W.W. and A. Stewart-Oaten. 1989. Aggregation by parasitoids and predators: effects on equilibrium and stability. Amer. Natur. 134: 288-310.

Murdoch, W.W., S.L. Swarbrick, R.F. Luck, S. Walde, and D.S. Yu. 1996. Refuge dynamics and metapopulation dynamics: a test. Amer. Natur. 147: 424-444.

Pulliam, H. R. 1988. Sources, sinks and population regulation. American Naturalist 132: 652-661.

Rohani, P., T.J. Lewis, D. Gruenbaum, and G.D. Ruxton. 1997. Spatial self-organization in ecology: pretty patterns or robust reality? Trends in Ecology and Evolution 12: 70-74.

Strogatz, S. 1994. Nonlinear Dynamics and Chaos. Perseus Books, Reading Mass.

Taylor, A.D. 1993. Heterogeneity in host-parasitoid interactions: 'aggregation of risk' and the '$CV^2 > 1$' rule. Trends in Ecology and Evolution 8: 400-405.

Tilman, D. 1982. Resource Competition and Community Structure. Princeton University Press, Princeton NJ.

Turchin, P. 2003. Complex Population Dynamics: a Theoretical/Empirical Synthesis. Princeton University Press, Princeton NJ.

Turchin, P., C.J. Briggs, S.P. Ellner, A. Fischlin, B.E. Kendall, E. McCauley, W.W. Murdoch, S.N. Wood. 2002. Population cycles of the larch budmoth in Switzerland. pp. 130-141 in: A. Berryman (ed.) Population Cycles. Oxford University Press.

Turchin, P., S.N. Wood, S.P. Ellner, B.E. Kendall, W.W. Murdoch, A. Fischlin, J. Casas, E. McCauley, C.J. Briggs. 2003. Dynamical effects of plant quality and parasitism on population cycles of larch budmoth. Ecology 84: 12071214.

Veilleux, B. G. 1976. The analysis of a predatory interaction between *Didinium* and *Paramecium*. Master's thesis, University of Alberta.

Veilleux, B. G. 1979. An analysis of the predatory interaction between *Paramecium* and *Didinium* Journal of Animal Ecology 4: 787-803.

Volterra, V. 1926. Fluctuations in the abundance of a species considered mathematically. Nature 118: 558-560.

Zimmer, C. 1999. Life after chaos. Science 284: 83-86.

4.9 Appendix: some matrix algebra

- A matrix is a rectangular array of numbers; a vector is a list of numbers.

- Addition of matrices or vectors is element-by-element (which requires that the items being added are the same size and shape); ditto subtraction, and multiplication of a vector or matrix by a

number. Examples:

$$\begin{aligned} \begin{bmatrix} 1 & 2 & 3 \\ 4 & 5 & 6 \end{bmatrix} + \begin{bmatrix} 2 & 6 & 10 \\ 4 & 8 & 12 \end{bmatrix} &= \begin{bmatrix} 1+2 & 2+6 & 3+10 \\ 4+4 & 5+8 & 6+12 \end{bmatrix} \\ 2\begin{bmatrix} 1 & 2 \\ 3 & 4 \end{bmatrix} = \begin{bmatrix} 2 & 4 \\ 6 & 8 \end{bmatrix} \qquad & 2[1,1,2,2] = [2,2,4,4] \end{aligned} \tag{4.61}$$

- Two vectors v, w of the same size, or two matrices of the same size, can be multiplied element-by-element to yield another vector or matrix. This is called the *Hadamard product* and is usually indicated by an open circle, $\circ$. Example:

$$(1,2,3) \circ (2,3,4) = (1 \times 2, 2 \times 3, 3 \times 4) = (2,6,12) \tag{4.62}$$

- The **dot product** or **inner product** of two vectors v, w of the same size is the sum of the entries in their product. Notation varies: $\langle v, w \rangle$, (v, w) and $v \bullet w$ are often used.

$$\langle (1,2,3), (2,3,4) \rangle = (1 \times 2 + 2 \times 3 + 3 \times 4) = (2 + 6 + 12) = 20. \tag{4.63}$$

Matrix-vector and matrix-matrix multiplication are **not** done element-by-element.

Matrix-vector multiplication: If $\mathbf{A}$ is a matrix and x a vector, then

$y = \mathbf{A}x$ is a vector whose i^{th} entry is $y[i] = \langle \mathbf{A}[i,], x \rangle$.

That is: to compute $\mathbf{A}x$, take the inner product of x with each row of $\mathbf{A}$, and combine those values into a vector. Consequently

- $\mathbf{A}x$ is only defined if the length of x equals the number of columns of $\mathbf{A}$
- The length of $\mathbf{A}x$ will equal the number of rows of $\mathbf{A}$
- In brief: an $m \times n$ matrix takes n-vectors to m-vectors.

$$\text{Example}: \begin{bmatrix} 1 & 2 & 3 \\ 4 & 5 & 6 \end{bmatrix} \begin{bmatrix} 1 \\ 3 \\ 5 \end{bmatrix} = \begin{bmatrix} \langle (1,2,3), (1,3,5) \rangle \\ \langle (4,5,6), (1,3,5) \rangle \end{bmatrix} = \begin{bmatrix} 1+6+15 \\ 4+15+30 \end{bmatrix} = \begin{bmatrix} 22 \\ 49 \end{bmatrix} \tag{4.64}$$

Here a 2×3 matrix (2 rows, 3 columns) has taken a 3-vector to a 2-vector.

We can see from the above that there is another, equivalent way to define matrix-vector multiplication: $\mathbf{A}x$ is the vector

$$(x[1] \times \text{1st column of } \mathbf{A}) + (x[2] \times \text{2nd column of } \mathbf{A}) + \cdots (x[n] \times \text{last column of } \mathbf{A}).$$

Matrix-vector multiplication is a **linear operation**. That is, if x, y are vectors and a, b are numbers, then

$$\mathbf{A}(ax + by) = a(\mathbf{A}x) + b(\mathbf{A}y) \tag{4.65}$$

and the same interchange of operations holds for any number of summed terms. This is a *very important property.* In fact, any linear operation on vectors can be expressed as multiplication by some matrix.

4.10 Appendix: complex numbers

Matrix eigenvalues are often complex numbers, so we need to know a bit about how these work. A complex number z consists of a *real part*, which is an ordinary real number, and an *imaginary part* which is a multiple of $i = \sqrt{-1}$; for example $3 + 5i$ has real part 3, and imaginary part $5i$.

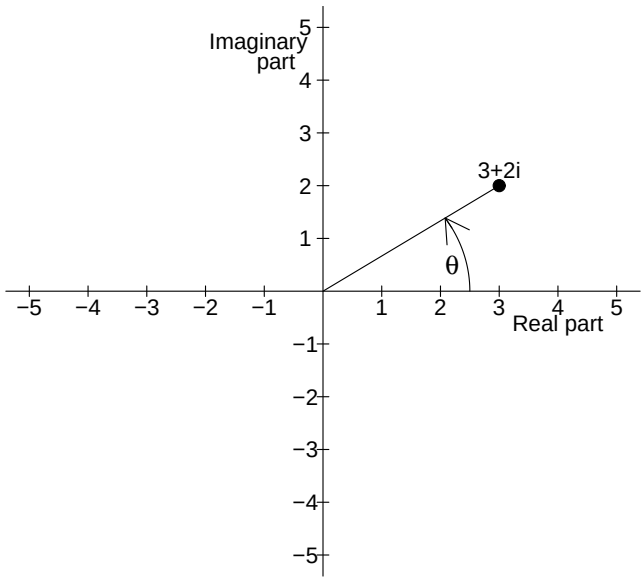

Figure 4.10: Representation of complex numbers as points in the plane.

Complex numbers can be visualized as points in the *complex plane* (Figure 4.10), with the real part on the horizontal axis, and imaginary part on the vertical. This depiction of complex numbers also clears up the question "what is the square root of -1, anyway?" Complex numbers are a way of taking the arithmetic operations on real numbers – addition, subtraction, multiplication and division – and defining them for points in the plane. $\sqrt{-1}$ is the vector such that you get -1 (i.e. $-1 + 0i$ in the complex plane) when you multiply that vector by itself.

The arithmetic of complex numbers is defined by treating them like ordinary numbers and applying the

rule $i^2 = -1$.

$$\begin{aligned}
(a+bi)+(c+di) &= (a+c)+(b+d)i \\
(a+bi)-(c+di) &= (a-c)+(b-d)i \\
(a+bi)\times(c+di) &= (a\times c)+(a\times di)+(bi\times c)+(bi\times di) \\
&= ac+(ad+bc)i+bd(-1) \\
&= (ac-bd)+(ad+bc)i
\end{aligned} \tag{4.66}$$

For division it is best to use an alternate representation for complex numbers using polar coordinates and the exponential function. Recall the Taylor series expansion

$$e^x = 1 + x + \frac{x^2}{2!} + \frac{x^3}{3!} + \frac{x^4}{4!} + \cdots .$$

Applying this to an imaginary number bi, and using the Taylor series for the sine and cosine functions, we get

$$\begin{aligned}
e^{bi} &= 1 + bi - \frac{b^2}{2!} - i\frac{b^3}{3!} + b\frac{x^4}{4!} + \cdots \\
&= (1 - \frac{b^2}{2!} + b\frac{x^4}{4!} - \cdots) + i(b - \frac{b^3}{3!} + \cdots) \\
&= \cos(b) + i\sin(b),
\end{aligned} \tag{4.67}$$

For a complex number $z = a + bi$ we then have

$$e^z = e^{a+bi} = e^a e^{bi} = e^a(\cos(b) + i\sin(b)) \tag{4.68}$$

Referring again to Figure 4.10, for any complex number z let r be the distance from the origion to z, and θ the counter-clockwise angle between the real axis and the line from z to the origin. Then the definitions of the cosine and sine functions give us

$$z = r(\cos(\theta) + i\sin(\theta)) = re^{i\theta}. \tag{4.69}$$

The relationships between the Cartesian representation $z = a + bi$ and the polar representation $z = re^{i\theta}$ are

$$\begin{aligned}
a = r\cos(\theta), \quad b = r\sin(\theta) \\
r = \sqrt{a^2+b^2}, \quad \theta = \tan^{-1}(b/a)
\end{aligned} \tag{4.70}$$

The quantity $r = \sqrt{a^2+b^2}$ is often called the *absolute value*, the *modulus* or the *magnitude* of the complex number $z = a + bi$, and θ is sometimes called the *argument*.

Finally, we can define division for complex numbers. If $z_1 = r_1 e^{i\theta_1}$, $z_2 = r_2 e^{i\theta_2}$, then

$$\frac{z_1}{z2} = \frac{r_1 e^{i\theta_1}}{r_2 e^{i\theta_2}} = \frac{r_1}{r_2}\frac{e^{i\theta_1}}{e^{i\theta_2}} = \frac{r_1}{r_2}e^{i(\theta_1-\theta_2)}. \tag{4.71}$$

The polar representation is also convenient for multiplication:

$$z_1 z_2 = r_1 e^{i\theta_1} \times r_2 e^{i\theta_2} = r_1 r_2 e^{i\theta_1} e^{i\theta_2} \quad = r_1 r_2 e^{i(\theta_1+\theta_2)}. \tag{4.72}$$

Stability analysis for differential equations leads to complex numbers of the form $e^{\lambda t}$ where $\lambda = a + bi$ is an eigenvalue of the Jacobian matrix. The behavior of these as $t \to infty$ is a combination of exponential

growth or decay, governed by the real part of λ, and sinusoidal oscillations whose rate depends on the imaginary part:

$$e^{\lambda t} = e^{(a+bi)t} = e^{at+bti} = e^{at}(\cos(bt) + i\sin(bt)), \tag{4.73}$$

which implies that

$$|e^{\lambda t}| = e^{at}.$$

So if $a > 0$ there is exponential growth of $e^{\lambda t}$ as $t \to \infty$, and if $a < 0$ there is exponential decay to 0.

This is one of the many reasons why complex numbers are useful. Solutions to linear dynamic models involve combinations of exponential growth/decay and sinusoidal oscillations (think of a damped pendulum, for example), and complex numbers allow us to express these together in a simple form and work with them using arithmetic operations that behave just like ordinary arithmetic.

Stability analysis for difference equations leads to complex numbers of the form λ^t where λ is an eigenvalue of the Jacobian matrix. In this case it is better to use the polar representation $\lambda = re^{i\theta}$:

$$\lambda^t = (re^{i\theta})^t = r^t e^{i\theta t} = r^t(\cos(\theta t) + i\sin(\theta t)). \tag{4.74}$$

which implies that

$$|\lambda^t| = r^t = |\lambda|^t.$$

So if $|\lambda| > 1$ there is exponential growth of λ^t, and if $|\lambda| < 1$ there is exponential decay to 0.

4.11 Appendix: Poisson distribution of eggs per host

The Poisson distribution for the numbers of parasitoid eggs per host can be derived by a limiting process. Imagine the habitat divided into n cells of size $1/n$, having chosen units so that the total habitat size is 1. In a time interval of length T, each parasitoid searches through cT units of area, consisting of ncT randomly chosen cells. There are a total of P parasitoids doing this, hence a total of $ncTP$ events of a parasitoid searching a cell and attacking any occupants. The number of attacks on any one host is equal to the number of searches through the cell that it's in. Under the assumption that parasitoids search randomly and independent of one another, the number of searches through any one cell is a Binomial random variable with $N = ncTP$ "trials" (the total number of searches by all parasitoids), and "success probability" $p = 1/n$ (the probability that the focal cell is chosen for search). The mean number of attacks on a given cell is $Np = cTP$. As $N \to \infty$, a Binomial(N, p) random variable with $Np = \lambda$ converges to a Poisson(λ) distribution. So as $n \to \infty$ the number of attacks on a given host converges to a Poisson random variable with mean cTP. Since each parasitoid searches an area of size c per unit time, cT is the parasitoid "area of discovery" that is denoted a in (4.39).